



Faculty of Science - University of Benghazi

Libyan Journal of Science &amp; Technology

journal home page: [www.sc.uob.edu.ly/pages/page/77](http://www.sc.uob.edu.ly/pages/page/77)

## Synthesis procedure and Physico-chemical characterization of supported Molybdenum oxide catalysts

Abdelhadi S. Benhmid <sup>a,\*</sup>, Khaled M. Edbey <sup>a</sup>, Ali F. Bukhzam <sup>a</sup>, Hend M. Alhowari <sup>a</sup>, Gamal. A. Mekhemer <sup>b</sup>, Mohamed I. Zaki <sup>b</sup>

<sup>a</sup>Chemistry department, Faculty of Science, Benghazi University, P.O. Box - 1308 Benghazi, Libya

<sup>b</sup>Chemistry department, Faculty of Science, Minia University, El- Minia, Egypt

### Highlights

- Particle size was found to be increase dramatically with increasing loading level of molybdenum oxide.
- High dispersion was displayed on silica supported molybdenum oxide catalyst at low loading level (3 and 5 wt%).
- There are at least three different molybdenum species present on the Al<sub>2</sub>O<sub>3</sub> surface under ambient conditions and their relative concentrations depend on the molybdenum oxide coverage.

### ARTICLE INFO

#### Article history:

Received 02 September 2017

Revised 10 March 2018

Accepted 11 September 2018

Available online 19 September 2018

#### Keywords:

Molybdenum oxide catalysts; XRD; Particle size, Ex-Situ FT-IR and Laser Raman Spectroscopy

\*Corresponding author:

E-mail address: [benhmid@hotmail.com](mailto:benhmid@hotmail.com)

A. S. Benhmid

### ABSTRACT

A series of alumina and silica supported molybdenum oxide catalysts has been prepared using ammonium heptamolybdate over a wide range of loading levels (3 – 20 wt% of molybdenum oxide) by the wet impregnating method. For a better understanding of the catalytic behaviour of the catalysts, the catalysts were characterised using different techniques like, XRD, FT-IR spectroscopy and Laser Raman spectroscopy. The XRD results of alumina supported molybdenum oxide exhibits the crystallinity of catalysts and particle size was found to increase with increasing the loading level of molybdenum oxide. The similar effect was observed in case of sulfated alumina supported molybdenum oxide (xMoAlS). However the XRD results in case of silica supported molybdenum oxide exhibits high dispersion at low loading level (3 and 5 wt%). The FT-IR results revealed that the dispersion capacity of molybdenum oxide from MoAlS is larger than of molybdenum oxide from MoAl. However, the ex-situ FT-IR spectra of MoSi and MoSiS catalysts showed that the dispersion capacity of molybdenum oxide from MoSiS is bigger than of molybdenum oxide from MoSi. Laser Raman spectroscopy studies demonstrated that there are at least three different molybdenum oxide species (tetrahedral and octahedral coordinated surface species as well as a crystalline MoO<sub>3</sub> phase) present on the Al<sub>2</sub>O<sub>3</sub> surface under ambient conditions and that their relative concentrations depend on the molybdenum oxide coverage. Laser Raman Spectroscopy of xMoAl catalysts indicated that the formation of molybdenum oxide of higher bond order in xMoAlS catalysts than in xMoAl catalysts.

© 2018 University of Benghazi. All rights reserved.

## 1. Introduction

Molybdena catalysts have been used for quite a long time. The term molybdena is used here to denote a composite catalyst consisting of molybdenum oxide supported on an activated support, commonly alumina. In early time, it was found that certain transition metals, particularly cobalt and nickel, promote the molybdena catalyst for hydrodesulfurization (HDS) reactions.

Cobalt molybdate catalyst has been used much in the petroleum industry for hydrotreating and hydrodesulfurization. More recently, these catalysts have been employed in chemical, petroleum, coal liquefaction, and pollution control industries (Mathew *et al.*, 2006; Haber *et al.*, 1981; El-Sharkawy *et al.*, 2007).

Transition metal oxides supported on oxide carriers are used specifically in the field of selective oxidation reactions. These catalysts are typically prepared by deposition of catalytically active molybdenum oxide component on the surface of an oxide support (TiO<sub>2</sub>, Al<sub>2</sub>O<sub>3</sub>, ZrO<sub>2</sub>, SiO<sub>2</sub> and MgO). The excessive flexibility of supported Mo-catalysts is related to the different molecular structures that molybdenum species can simultaneously possess when supported and to the ability of Mo atom to assume various oxidation states, depending on the pre-treatment and/or the reaction atmosphere (Mathew *et al.*, 2006). It is well-known catalysts based on multi component oxides exhibit a better performance rather than when component oxide were used separately (Thiemann *et al.*,

2011). Molybdenum supported on oxides such as  $\gamma$ -alumina, silica and alumina-silica is widely used in such petroleum refining processes as Hydro treating or Hydro cracking (Banares *et al.*, 1994).

Alumina is very commonly used support for molybdenum. In recent years, alumina supported catalysts have attracted appreciable attention due to their industrial and technological application. Many studies devoted for understand the nature of interaction of molybdenum species with alumina support (Mathew *et al.*, 2006; Mulcahy *et al.*, 1990; Spanose *et al.*, 1990).

The molybdena has a very high dispersion in MoO<sub>3</sub>/ $\gamma$ -Al<sub>2</sub>O<sub>3</sub> catalysts. The molybdena forms monolayer on  $\gamma$ -Al<sub>2</sub>O<sub>3</sub> surface. During the impregnation and calcination steps, the molybdena is fixed on Al-OH groups forming Al-O-Mo bonds (Ng *et al.*, 1985). In the presence of low amounts of MoO<sub>3</sub> ( $\leq 4$  wt%) the formation of isolated, tetrahedrally coordinated [MoO<sub>4</sub>] species is preferred. High molybdena loadings or thermal treatment favours the formation of polymeric molybdate structures in which the Mo(VI) ion is octahedrally coordinated.

Previous studies have shown that catalytic properties may depend on the molybdenum oxide structure as well as the choice of the support material (Banares *et al.*, 1995; Leyrer *et al.*, 1990). For a detailed understanding of supported molybdenum oxide catalysts one strategy may be to separate the effects of molybdenum oxide structure from those of support material. Silica seems to be

the material of choice considering its weak interaction with molybdenum oxide. The relatively inert of silica the detailed state of the deposited supported molybdenum oxide may still depend on variety of parameter such as silica material and its pre-treatment, the synthesis procedure. For highly dispersed molybdenum oxide supported on silica a hydrated and a dehydrated state have to be distinguished.

The hydrated state is present when the sample is revealed to moisture under ambient condition. If the sample is treated in dry synthetic air at elevated temperature ( $\geq 350^\circ\text{C}$ ), the molybdenum oxide is converted into a dehydrated state (Leyrer et al., 1986). Generally, it has been found that alumina-supported  $\text{MoO}_3$  catalysts of a high dispersion can be obtained up to high loadings, however the formation of  $\text{MoO}_3$  crystallites occurs at significantly lower loadings in case of  $\text{SiO}_2$  supported catalysts (Kakuta et al., 1988; Sarrazin et al., 1989). The difference in interaction between the metal precursor (usually from ammonium heptamolybdate (AHM)), dissolved in water and the alumina and silica supports brings about the difference in dispersion. The interaction between the precursor and the support depends on the sign of the surface charge of the support and of the dissolved complexes of precursor. It has been observed that the interaction between the anionic heptamolybdate clusters and the positively charged  $\text{Al}_2\text{O}_3$ -surface is better than between the clusters and the  $\text{SiO}_2$ -surface, which is negatively charged. This leads to spreading of the molybdena phase over  $\text{Al}_2\text{O}_3$ . Because of the lack of interaction between heptamolybdate and  $\text{SiO}_2$  formation of  $\text{MoO}_3$  crystallites in  $\text{MoO}_3/\text{SiO}_2$  catalyst occurs at low loading (Kakuta et al., 1988; Sarrazin et al., 1989; Stencil et al., 1986). During drying and calcination, these crystallites have a tendency to more coalescence due to the high solubility of hexavalent molybdenum species in water, and volatility of  $\text{MoO}_2(\text{OH})_2$ . Subsequently, the dispersion of silica-supported catalysts is not very stable and usually these catalysts show bulk  $\text{MoO}_3$  features in catalytic test reaction.

However, there is still significant scope for the determination of the physicochemical properties, the nature of the support and its pore structure. Other parameters such as the loading level of the active component and the nature and concentration of promoters will be of interest. In order to achieve these objectives, the following steps are carried out:

- Preparation of supported molybdena at various loading levels using two different supports ( $\text{SiO}_2$  and  $\text{Al}_2\text{O}_3$ ) by the impregnation method, subsequent drying at  $120^\circ\text{C}$  and calcinations at  $600^\circ\text{C}$  in air.
- Characterization of surface structures assumed by the supported molybdena species by means ex-Situ FT-IR, Laser Raman Spectroscopy and XRD.

## 2. Experimental

### 2.1. Catalyst preparation

High purity ammonium heptamolybdate  $(\text{NH}_4)_6\text{Mo}_7\text{O}_{24}\cdot 4\text{H}_2\text{O}$ , Merck, was used as precursor for supported and unsupported  $\text{MoO}_x$  catalysts. High surface area ( $100 \pm 10 \text{ m}^2/\text{g}$ ) aluminium oxide of Degussa AG (Frankfurt, Germany) was used as carrier for supported catalysts. The material bulk was examined by x-ray diffraction to assume a crystalline structure largely similar to that of  $\gamma$ -modification (ASTM Card No. 10-425). Silica ( $200 \pm 10 \text{ m}^2/\text{g}$ ), the other catalyst support material, was also a Degussa product. It is commercially known as Aerosil-200. According to the manufacturer, it is void of particle porosity. In addition, it is amorphous to x-ray diffraction.

#### 2.1.1. Unsupported molybdenum oxide

Unsupported molybdenum oxide was obtained by calcinations of ammonium heptamolybdate (AHM) at  $550^\circ\text{C}$  in a static atmosphere of air for 3 h.

#### 2.1.2. Supported molybdenum oxide

Supported molybdenum oxide samples were prepared by wet impregnation method (Simionato et al., 2003), using alumina and silica as support materials and aqueous solution of AHM as the impregnating solution. The impregnation solution was prepared by dissolving a calculated amount of the precursors AHM of the required loads 3, 5, 10, 15 and 20 wt%  $\text{MoO}_3$  in the final supported oxide materials in a suitable volume of distilled water (50 cc/g support).

The support powder particles were sprayed slowly onto the impregnation solution, while being continuously stirred. The free water was removed by evaporation at  $120^\circ\text{C}$  for 1 h. The AHM impregnated support material thus yield was dried at  $120^\circ\text{C}$  for 24 h in an oven. Supported molybdenum oxide on alumina (xMoAl) and silica (xMoSi) were obtained by calcinations at  $550^\circ\text{C}$  for 3 h in air of the corresponding impregnated supports. The resulting catalysts were kept dry on  $\text{CaCl}_2$ , until further use. For convenience, the various catalysts are denoted below by 3MoAl indicates the 3 wt%- $\text{MoO}_3$  loaded alumina supported molybdenum oxide catalyst, whereas 3MoSi indicates the 3 wt%- $\text{MoO}_3$  loaded silica supported molybdenum oxide catalyst.

Sulfated catalysts were prepared from alumina and silica supported  $\text{MoO}_3$  catalysts (xMoAl and xMoSi) by impregnation with ammonium sulfate. The impregnation was carried out by immersing the dried supported catalysts (xMoAl or xMoSi) in an aqueous solution containing a desired amount of  $(\text{NH}_4)_2\text{SO}_4$  and evaporating to dryness, followed by calcining similarly as in case of supported catalysts. The supported catalysts promoted with sulfate were designated as xMoAlS or xMoSiS. The amount of sulfate adsorbed on supported catalysts after impregnation and before calcinations is approximately 6 wt%  $\text{SO}_4^{2-}$ .

### 2.2. Characterization of catalysts

All the catalytic materials as prepared in the previous sections were thoroughly characterized for their surface and bulk properties by appropriate techniques as indicated below:

Crystallinity and particle size by Powder X-ray diffraction (PXRD), dispersion capacity by Fourier Transform Infrared spectrophotometry (FTIR) and molecular composition and structure within a species by Laser Raman spectroscopy

#### 2.2.1. X-ray diffraction

The X-ray powder diffractometry patterns were obtained, using Ni-filtered  $\text{CuK}\alpha$ -radiation ( $\lambda=1.54056 \text{ \AA}$ ); on a JSX-60 PA Jeol X-ray spectrometer. The generator at 35 KV and 20 mA, and the diffractometer at  $2\theta$  diverging and receiving slits and at a scan rate of 20 mm/min. The sample ground to a particle size less than  $44 \mu$  and packed into the wall of a sample holder, and then mounted in a horizontal position. We identified the crystalline phases by referring to the ASTM data files (Smith, 1960). Crystallite sizing ( $D_{hkl}$ ) was carried out using the line broadening technique in conjunction with Scherrer's formula (Mercera et al., 1990).

#### 2.2.2. Fourier Transform infrared spectroscopy

The Fourier Transform Infrared spectrophotometry, the Ex-situ FT-IR spectra of supports, unsupported and supported catalysts were taken at frequency range  $4000\text{--}400 \text{ cm}^{-1}$  with  $4 \text{ cm}^{-1}$  resolution using a Genesis-II FT-IR Mattson spectrophotometer (USA) and an online PC with win first Lite (V 1.02) software for spectra acquisition and handling. The spectra were taken for thin ( $>20 \text{ mg/cm}$ ) lightly loaded ( $>1 \text{ wt\%}$ ) wafer of KBr-supported test samples. About 1–2 mg of the catalyst as a fine powder was mixed well with spectroscopy pure KBr powder and was finally grinded in agate mortar.

#### 2.2.3. Laser Raman spectroscopy

The Laser Raman spectroscopic experiments, ca. 90 mg of the catalyst was pressed into pellets, of 5 mm diameter and 0.8 mm

thickness. The catalyst as pellets was heated (5°C/min) in stream of O<sub>2</sub> (40 ml/min) at 500°C for 1 h to remove the contaminated carbonates and organic materials. The spectra were recorded at room temperatures. The Raman spectra was recorded over range characteristics to the structure of SO<sub>4</sub><sup>2-</sup> and molybdenum oxide, the range at 1200–100 cm<sup>-1</sup> on a computer controlled Dilor OMARS89 spectrometer which was equipped with an optical multichannel analyser (OMA) Model IRY12 From Spectroscopy Instrument. The excitation line was at 488 nm from an Ar ion Laser. For a given spectrum, the excitation power at the sample was constant. The Raman spectra were measured with up to 5 cm<sup>-1</sup> spectral resolution with an absolute accuracy of ±1 cm<sup>-1</sup>.

### 3. Results and Discussion

The results obtained from various characterization techniques and catalytic behavior studies and detailed discussions on these results are presented as follows:

#### 3.1. X-ray diffraction (XRD)

X-ray powder diffraction of alumina, molybdena and supported molybdena catalysts (xMoAl), pure silica and silica supported molybdenum oxide (xMoSi) at different loading levels are discussed below.

##### 3.1.1. XRD of alumina supported molybdenum oxide

X-ray powder diffraction of alumina, molybdena and supported molybdena catalysts (xMoAl) at different loading levels are shown in Fig. 1. The XRD patterns of alumina displays a few weak broad peaks which are indicative of fine crystallites of the  $\gamma$ -Al<sub>2</sub>O<sub>3</sub> phase (JCPDS 29–1486). The average crystallite size derived from the peak width at half maximum (PWHM) was ca. 10.3±1 nm (Table 1). The pattern of pure molybdenum oxide (MoO<sub>3</sub>) found to be highly crystalline and exhibited several sharp peaks (Fig. 1).

X-ray diffractograms of the calcined products of supported catalysts xMoAl at 550°C for 3 h at different loading levels samples are also shown in Fig. 1. The XRD patterns of 3MoAl and 5MoAl catalysts display the XRD pattern of  $\gamma$ -Al<sub>2</sub>O<sub>3</sub> structure. This means that MoO<sub>3</sub> will have high dispersed on alumina until 5 wt% of MoO<sub>3</sub>. The XRD pattern of 10MoAl display peaks characteristic to bulk MoO<sub>3</sub> was formed. These peaks become more intense as the molybdenum oxide content of catalyst increased. The molybdena has a very high dispersion in MoO<sub>3</sub>/ $\gamma$ -Al<sub>2</sub>O<sub>3</sub> catalysts at low loading level (3, 5MoAl). In the presence of low amounts of MoO<sub>3</sub> ( $\leq 3$  wt%) the formation of the isolated tetrahedrally coordinated [MoO<sub>4</sub>] species is preferred. However, the samples with a higher proportion of molybdena contents favour the formation of polymeric molybdate structures in which the Mo(VI) ion is octahedrally coordinated. Crystalline molybdena is usually observed when the molybdena amounts is higher than 15 wt% and Al<sub>2</sub>(MoO<sub>4</sub>)<sub>3</sub> formation (Henker et al., 1991). The difference in the XRD patterns of the supported catalyst from that of pure support and molybdena is an indication of much strong molybdena-support interaction.

The data reported in Table 1 reveal that the particle size obtained from XRD data of alumina supported molybdenum oxide catalysts increases dramatically with increasing the molybdena content.

The XRD diffractogram of sulfated alumina supported molybdena catalysts (xMoAlS) are shown in Fig. 2. The XRD patterns of xMoAlS display peaks at low loading levels (3MoAlS) characteristic to bulk MoO<sub>3</sub> formation. These peaks increase with increasing the MoO<sub>3</sub> loaded, which lead to the increases the bulk of MoO<sub>3</sub>. The data obtained from XRD indicated that the presence of sulfate ion found to enhance the formation of MoO<sub>3</sub> at low loading level (3MoAl). In addition, the particle size of these catalysts increases with increasing of molybdena content (Table 1).

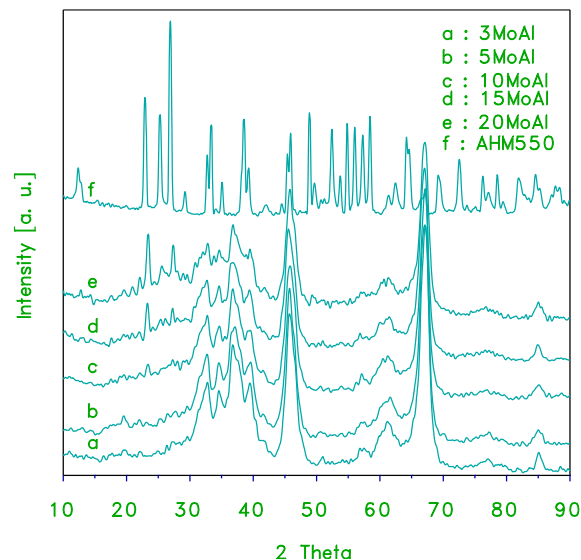


Fig. 1. X-ray powder diffractograms for xMoAl catalysts. Diffractograms of the support and unsupported MoO<sub>3</sub> are inset for comparison.

Table 1

Particle size obtained from XRD data of alumina supported molybdenum oxide at different loading levels and sulfated catalysts.

Samples	Particles size (D = 1 nm)
Al	10.3
MoO <sub>3</sub>	38.4
3MoAl	16.1
5MoAl	16.1
10MoAl	20.2
15MoAl	23.4
20MoAl	26.1
3MoAlS	14.1
5MoAlS	15.6
10MoAlS	17.3
15MoAlS	21.4
20MoAlS	23.3

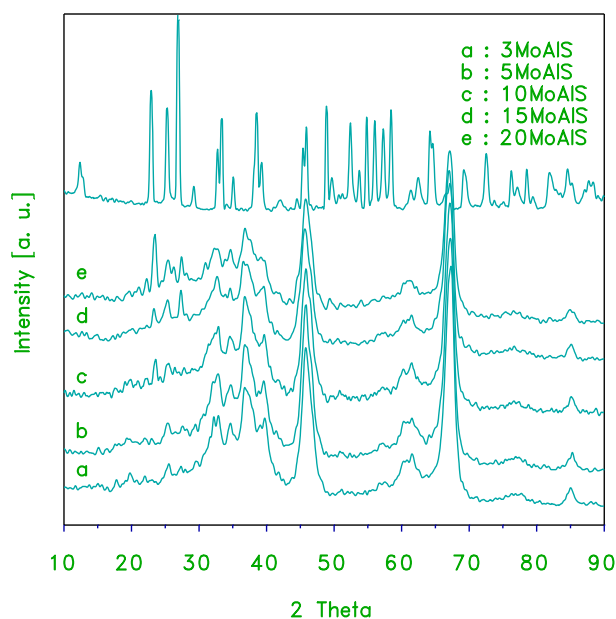
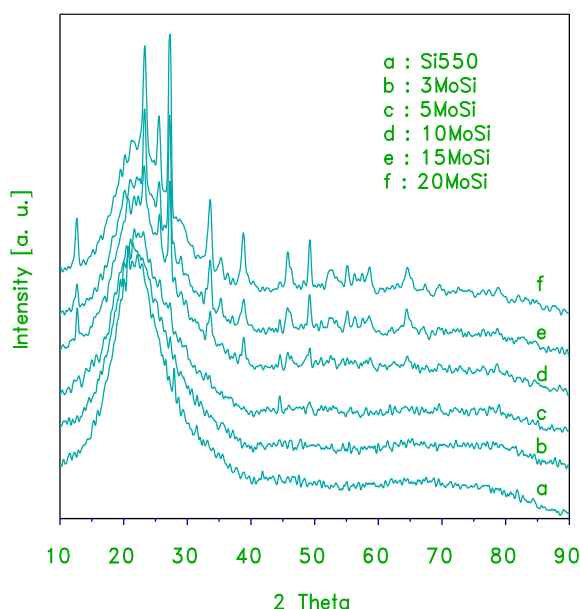


Fig. 2. X-ray powder diffractograms for xMoAlS catalysts. Diffractograms of the support and unsupported MoO<sub>3</sub> are inset for comparison.

### 3.1.2. XRD of silica supported molybdenum oxide

X-ray powder diffraction of pure silica and silica supported molybdenum oxide (xMoSi) at different loading levels are shown in Fig. 3. The XRD patterns of silica displays a broad peak due to non-crystalline silica (amorphous). The diffractograms of 3MoSi displays dominantly peak due to support (silica), and well-defined peaks that can be found in the diffractogram of MoO<sub>3</sub>. It was observed that the MoO<sub>3</sub> species was highly dispersed on silica at 3 and 5 wt% loaded. This result indicates that molybdena species are not crystallized but highly dispersed or exist as amorphous phase without possibility to know if the absence of any diffraction peak was due to absence of long-range order of MoO<sub>3</sub> or to low amount of MoO<sub>3</sub> to observe diffraction (Aritani et al., 2001; Gervasini et al., 2012). While at higher loading levels (10 wt%) the formation of MoO<sub>3</sub> bulk starts to be appeared. The formation of bulk molybdena increases with increasing the loading levels.



**Fig. 3.** X-ray powder diffractograms for xMoSi catalysts. Diffractograms of the support and unsupported MoO<sub>3</sub> are inset for comparison.

The patterns at highest loading levels 10, 15 and 20MoAl reveals the main presence of stable phase MoO<sub>3</sub> orthorhombic crystal structure appeared at higher loading (Gong et al., 2004). The particle size of these catalysts is found to be increased with further increasing the loading level of molybdenum oxide (Table 2).

X-ray diffractograms of sulfated silica supported molybdena catalysts at different loading levels are shown in Fig. 4. The diffractogram pattern exhibited by 3- and 5MoSiS is similar to that presented above for 3- and 5MoSi (Fig. 3) clearly display high dispersion of MoO<sub>3</sub> at these loading levels. Also, at higher loading levels  $\geq 10$  wt% the crystalline MoO<sub>3</sub> was increased. The results of particle size obtained from XRD data of silica supported molybdenum oxide at different loading levels and sulfated catalysts are given in Table 2. It can be shown from the table that the particle size of xMoSiS samples increases with increasing the loading levels up to 20 wt%.

**Table 2**

Particle size obtained from XRD data of silica supported molybdenum oxide at different loading levels and sulfated catalysts

Samples	Particles size (D=1 nm)
MoO <sub>3</sub>	38.4
10MoSi	25.4
15MoSi	28.3
20MoSi	33.4
10MoSiS	23.3
15MoSiS	25.8
20MoSiS	31.4

### 3.2. Ex-situ FT-IR spectra of catalyst

The Ex-situ FT-IR spectra of alumina supported molybdenum oxide and silica supported molybdenum oxide are discussed below.

#### 3.2.1 Ex-situ FT-IR spectra of alumina supported molybdenum oxide

Ex-situ FT-IR spectroscopic analysis of the supported catalysts were performed to get deep insight about the surface molybdenum oxide. Fig. 5 provides a comparison of the IR spectra obtained for the xMoAl samples, with those exhibited by alumina and molybdenum oxide. The spectrum of pure alumina displays two broad absorptions centered at 760 and 569 cm<sup>-1</sup> in common. These frequencies may attribute to the Al-O lattice vibrations of Al<sub>2</sub>O<sub>3</sub> (Gadsden et al., 1975).

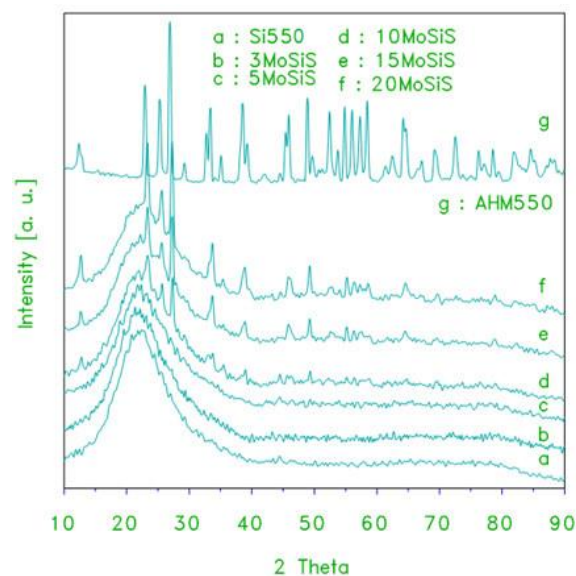


**Fig. 4.** X-ray powder diffractograms for xMoSiS catalysts. Diffractograms of support and unsupported MO<sub>3</sub> are inset for comparison.

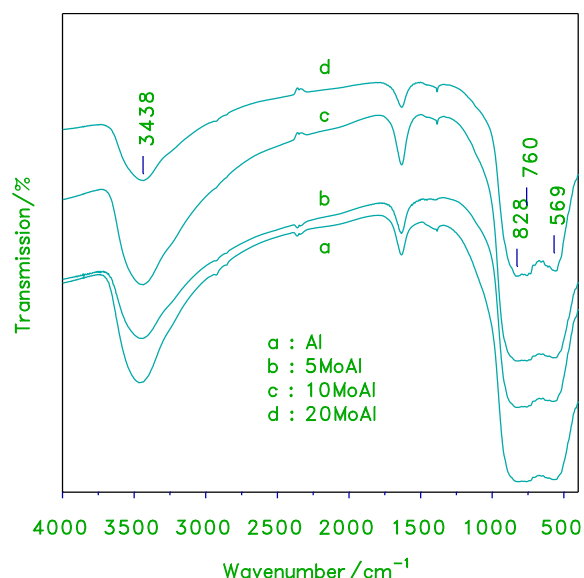


**Fig. 5.** FT-IR transmission spectra obtained for molybdenum oxide, the indicated set of \*alumina supported molybdenum oxide.

Alumina support also exhibited O-H stretching band at 3438 cm<sup>-1</sup> indicating the presence of basic hydroxyls, and similar stretching band of supported catalyst exhibited in the range 3600 to 3200 cm<sup>-1</sup>. As the loading level of molybdenum oxide is increased, the two broad bands 828, 569 cm<sup>-1</sup> decrease. The broad band of absorption indicated the formation of molybdenum oxide. As there was overlapping of Al-O bending vibration band in the

range 828, 760 and 569  $\text{cm}^{-1}$  with Mo=O band in supported catalysts (Henker et al., 1991), association of Mo-O with Al-O was clearly indicated by the intensity and shift of bands in the lower region (Mathew et al., 2006).

The IR spectra of sulfated xMoAlS catalysts (Fig. 6), shows the similar spectra of xMoAl in Fig. 5, the difference in spectra of xMoAlS loading level of sulfated xMoAlS increase become much strong absorptions at 828, 614 and 558  $\text{cm}^{-1}$ , which resembling those shown for MoO<sub>3</sub> surface species in the spectra of alumina supported molybdenum oxide and intensity of three bands are more intense than the spectra of xMoAl catalysts. This indicates that the formation of molybdenum oxide of higher bond order in xMoAlS catalysts than in xMoAl. Hence, the above IR spectral results are in a good agreement with the XRD results. By increasing the loading level of molybdenum oxide on alumina the crystallinity of MoO<sub>3</sub> increases dramatically. All the results discussed above clearly shows the dispersion capacity of molybdenum oxide from MoAlS is larger compared with molybdenum oxide from MoAl.

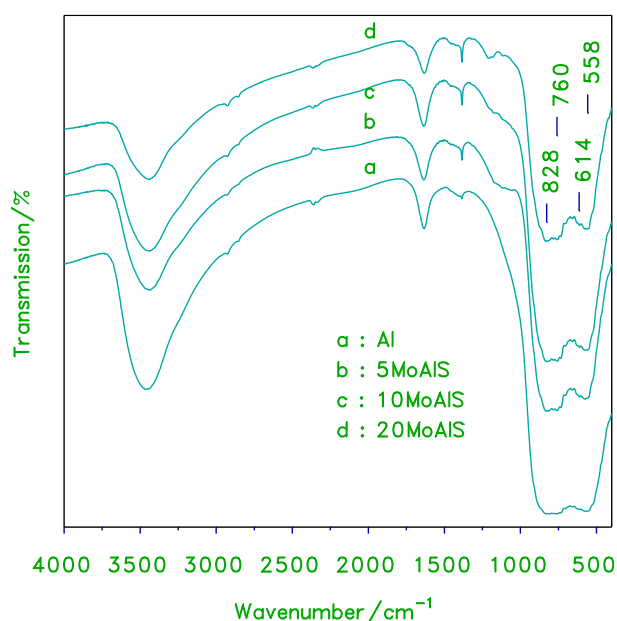


Fig. 6 FT-IR transmission spectra the obtained for molybdenum oxide and the indicated set of sulfated xMoAlS

### 3.2.2. Ex-situ FT-IR spectra of silica supported molybdenum oxide

Ex-situ FT-IR spectroscopic analysis of the supported catalysts were performed to get deep information about the surface molybdenum oxide. Fig. 7 provides a comparison of the IR spectra obtained for the xMoSi samples, with those exhibited by silica and molybdenum oxide. IR spectrum of pure silica display one broad absorption band centered at 1090  $\text{cm}^{-1}$ , and the other two absorption bands centered at 795 and 499  $\text{cm}^{-1}$ . These frequencies attributed to the Si-O lattice vibrations of SiO<sub>2</sub>. Water shows an intense characteristic broad absorption band centered at 3450  $\text{cm}^{-1}$  assigned to O-H stretching in H-bonding (Beganskiene et al., 2004). IR spectrum display strong absorption at 499  $\text{cm}^{-1}$  due to Mo-O lattice vibrations of molybdena phase (Al-Hajji, 2003). As the loading level of molybdenum oxide is increased, the absorption gradually narrow with the emergence of much strong absorption resembling the shown for MoO<sub>3</sub> surface species in the spectra of silica supported molybdenum oxide (Fig. 7). The intensities of these vibration bands increase with increasing the loading level of molybdenum oxide due to the increase in the formation of MoO<sub>3</sub>. There is an overlapping of Si-O bending vibration band in the range 795  $\text{cm}^{-1}$  with M=O band in supported catalysts.

The IR spectra of the sulfated, xMoSiS, samples (Fig. 8) is similar to the spectra of MoSi, which are shown in Fig. 7, with differences in an intensity absorption exhibits increase in absorption

with increase of loading of xMoSiS in range 499  $\text{cm}^{-1}$ , the increase in intensity is indicated to increase in formation of MoO<sub>3</sub>. Hence, the above IR spectral results in a good agreement with the XRD results. It has been noted that by increasing the loading level of molybdenum oxide on silica the crystallinity of MoO<sub>3</sub> dramatically increases.

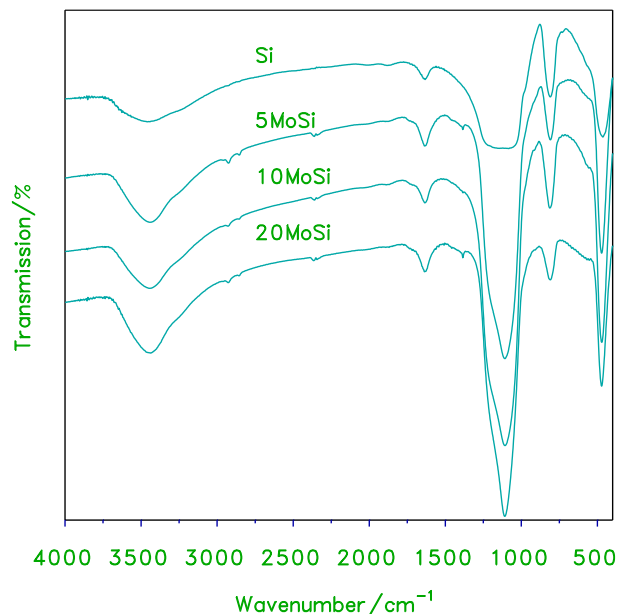


Fig.7. FT-IR transmission spectra obtained for molybdenum oxide, the indicated set of silica supported molybdenum oxide.

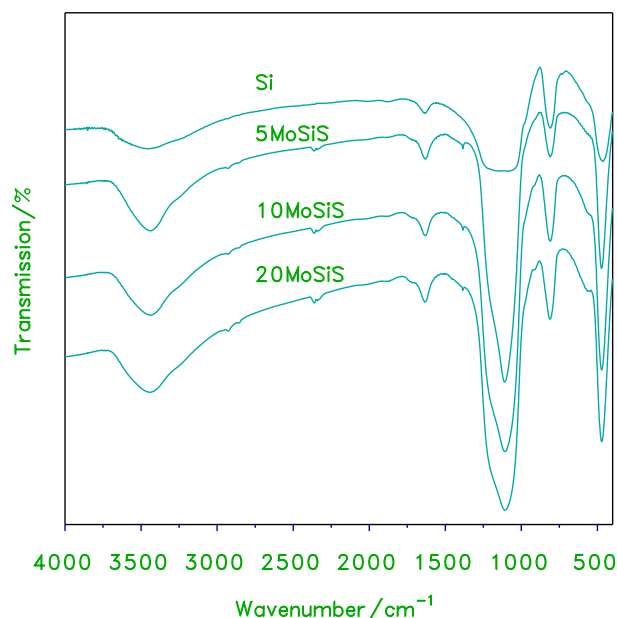


Fig. 8. FT-IR transmission spectra the obtained for molybdenum oxide and the indicated set of sulfated xMoSiS.

### 3.3. Laser Raman spectra of catalysts

Laser Raman spectroscopic analysis of the supported catalysts were performed to get deep information about the surface of molybdenum oxide.

#### 3.3.1. Laser Raman spectra of alumina supported molybdenum oxide catalysts

The result of the Laser Raman spectra obtained for the xMoAl samples at different loading levels presented in Fig. 9. All catalysts display bands at 956  $\text{cm}^{-1}$  (Mo=O stretching) at low molybdenum loading (5MoAl) tetrahedrally coordinated species (MoO<sub>4</sub><sup>2-</sup>) are present as small amount. With increasing the MoO<sub>3</sub> loading (10 MoAl) formation of new bands appear at 222 and 356  $\text{cm}^{-1}$  to

375  $\text{cm}^{-1}$  (Mo=O bending) and 834, 900  $\text{cm}^{-1}$  (asymmetric Mo-O-Mo stretching) and shift to higher values of bands 956 and 997  $\text{cm}^{-1}$  this shift can be attributed to a decrease in the bond strength of O-Mo-O groups that are joined to the support, because the high surface density of  $\text{MoO}_3$  species present in this catalyst, while at moderate loadings (between 5 and 20 wt%  $\text{MoO}_3$ ), tetrahedrally coordinated  $\text{MoO}_x$  species are present at 5MoAl catalyst (Mathew et al., 2006). Moreover, with increasing the amount of molybdenum oxide at 10MoAl the octahedrally coordinated species can be observed or more crystalline. The Raman spectra of sulfated, xMoAlS catalysts (Fig. 9) shows the similar spectra of xMoAl, but the difference in spectra of xMoAlS loading level become much strong absorptions at 853, 900 and 956  $\text{cm}^{-1}$ , which resembling those shown for  $\text{MoO}_3$  surface species in the spectra of alumina supported molybdenum oxide, and intensity of three bands are more intense than the spectra of xMoAl catalysts. This indicates that the formation of molybdenum oxide of higher bond order in xMoAlS catalysts than in xMoAl.

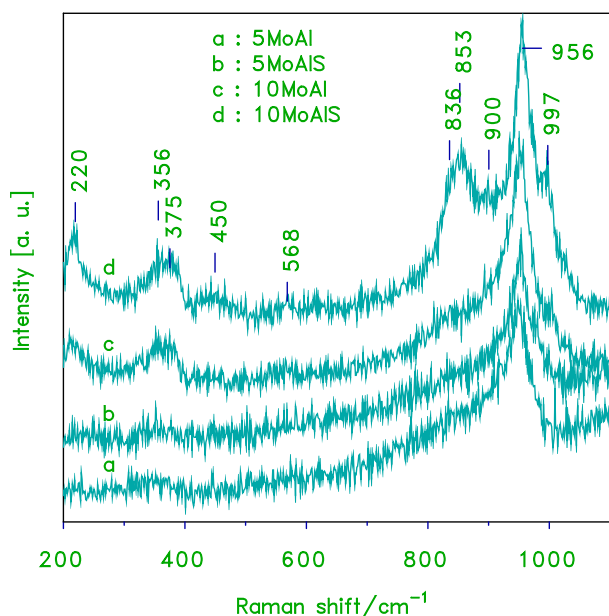


Fig. 9. Laser Raman spectra of alumina supported molybdenum oxide catalysts with sulfated xMoAlS catalysts

### 3.3.2. Laser Raman spectra of silica supported molybdenum oxide catalysts

Fig. 10 show a comparison of the Laser Raman spectra obtained for the xMoSi samples, with those exhibited by silica and molybdenum oxide. At low loading (5MoSi), the presence of  $\text{MoO}_3$  as a dispersed on the surface of 5MoSi exhibits two small vibrational bands at 816 and 992  $\text{cm}^{-1}$  of molybdena. The appeared bands indicate that they have small effect on the formation of molybdenum oxide (Boer et al., 1991). By increasing  $\text{MoO}_3$  loaded for 10 wt% become more intensive with increasing of intensity and new bands appears at 216 and 241  $\text{cm}^{-1}$ . The new bands can be assigned to molybdenyl bending as isolated and the Mo=O stretching mod shifts from 281 to 289  $\text{cm}^{-1}$  and at 666  $\text{cm}^{-1}$  (the shift and the change of band shape of the molybdenyl vibration can be interpreted as an indication that the two bands belong to at least two different contribution of the present molybdenum oxide species) and the presence of two sharp bands indicates that the surface molybdenum oxide species (Thielemann et al., 2011; McEvoy et al., 2005). At higher loading levels the characteristic bands of crystalline  $\text{MoO}_3$  are clearly observed.

The Raman spectra of the sulfated, xMoSiS catalysts (Fig. 10) displays similar to the spectra of MoSi with differences in an intensity absorption exhibits increase in absorption and sharper with increase loading of xMoSiS in range 816 and 992  $\text{cm}^{-1}$  indicates increase in formation of  $\text{MoO}_3$  crystalline. Hence, the above IR spec-

tral results are in a good agreement with the XRD results. By increasing the loading level of molybdenum oxide on alumina the crystallinity of  $\text{MoO}_3$  increases dramatically. All the results discussed above clearly shows the dispersion capacity of molybdenum oxide from MoAlS is larger compared with molybdenum oxide from MoAl.

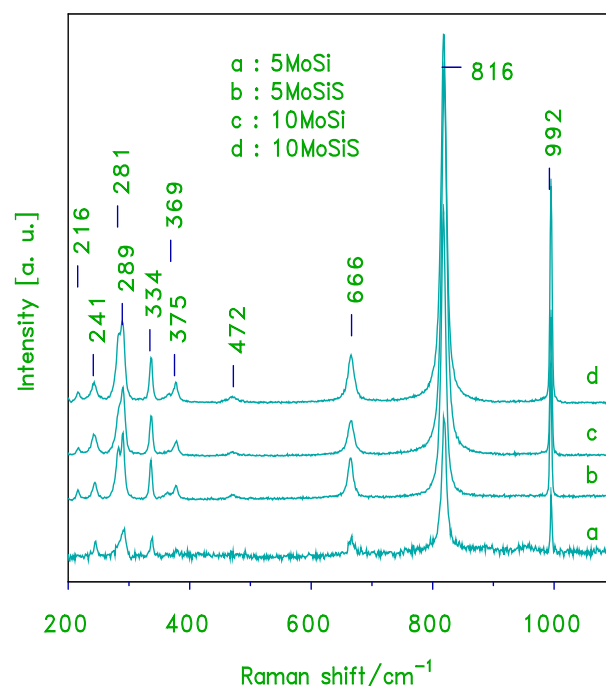


Fig. 10. Laser Raman spectra of silica supported molybdenum oxide catalysts with sulfated xMoSiS catalysts.

## 4. Conclusions

XRD results of alumina supported molybdenum oxide exhibits the crystallinity of catalysts and particle size are found to be increase with increasing the loading level of molybdenum oxide. Similar effect was observed in case of sulfated alumina supported molybdenum oxide (xMoAlS). XRD results of silica supported molybdenum oxide exhibits high dispersion at low loading level (3 and 5 wt%) whereas at higher loading levels the crystallinity and particle size increase with increasing loading level of molybdenum oxide. Sulfate catalysts of (xMoSi) show the similar effect. The FT-IR spectroscopic results were revealed that the dispersion capacity of molybdenum oxide from MoAlS is larger than of molybdenum oxide from MoAl. Whereas FT-IR spectra of MoSi and MoSiS catalysts show the dispersion capacity of molybdenum oxide from MoSi is bigger than of molybdenum oxide from MoSi. The Laser Raman Spectroscopy results of xMoAl catalysts clearly show the formation of molybdenum oxide of higher bond order in xMoAlS catalysts than in xMoAl catalysts. The laser Raman spectroscopy studies demonstrated that there are at least three different molybdenum oxide species (tetrahedral and octahedral coordinated surface species as well as a crystalline  $\text{MoO}_3$  phase) present on the  $\text{Al}_2\text{O}_3$  surface under ambient conditions and that their relative concentrations depend on the molybdenum oxide coverage, additionally Laser Raman Spectroscopy of xMoSi catalysts indicated that the higher intensity absorption (sharp) increase with increasing of loading level of Mo (xMoSi and xMoSiS) which indicate the formation of crystalline  $\text{MoO}_3$ .

## References

- Al-Hajji, L. A., Hasan, M. A., Zaki, M. I. (2003) 'Kinetic and characterization studies of the formation of barium monomolybdate in equimolar powder mixture of  $\text{BaCO}_3$  and  $\text{MoO}_3$ ', *J. Mater. Res.*, 18(10), pp. 2339-2349.

- Aritani, H., Fukuda, O., Miyaji, A., Hasegawa, S. (2001) 'Structural change of molybdenum on silica-alumina in contact with propene studied by ESR and Mo LIII-edge XANES', *Appl. Sur. Sci.*, 180, pp. 261-269.
- Banares, M. A., Hu, H., Wachs, I. E. (1994) 'Molybdena on Silica Catalysts: Role of Preparation Methods on the Structure-Selectivity Properties for the Oxidation of Methanol', *J. Catal.*, 150, pp. 407-420.
- Banares, M. A., Hu, H., Wachs, I. E. (1995) 'Genesis and Stability of Silicomolybdic Acid on Silica-Supported Molybdenum Oxide Catalysts: In-Situ Structural-Selectivity Study on Selective Oxidation Reactions', *J. Catal.*, 155, pp. 249-255.
- Beganskiene, A., Sirutkaitis, V., Kurtinaitiene, M., Juskenas R., Kareiva, A. (2004) 'FTIR, TEM and NMR investigations of Stöber silica nanoparticles', *Mater. Sci.*, 10(4), pp. 287-290.
- De Boer, M., Dillen, A. J., Koningsberger, D. C., Geus, J. W. (1991) 'Remarkable spreading behavior of molybdena on silica catalysts. An in situ EXAFS-Raman study', *Catal. Lett.*, 11, pp. 227-239.
- El-Sharkawy, E. A., Khder, A. S., Ahmed, A. I. (2007) 'Structural characterization and catalytic activity of molybdenum oxide supported zirconia catalysts', *Microporous and Mesoporous Materials*, 102, pp. 128-137.
- Gadsden, J. (1975) *An Infrared Spectra of Minerals and Related Inorganic Compounds*, Butterworths, London.
- Gervasini, A., Wahba, L., Finol M. D., Lamonier, J. F. (2012). 'Property and Activity of Molybdates Dispersed on Silica Obtained from Various Synthetic Procedures', *Mater. Sci. Appl.*, 3, pp. 195-212.
- Haber, J. (1981) *The Role of Molybdenum in Catalysis*, Climax Molybdenum Co., Ann Arbor, MI.
- Henker, M., Wendlandt, K. P., Valyon, J., Bornmann, P. (1991). 'Structure of MoO<sub>3</sub>/Al<sub>2</sub>O<sub>3</sub>-SiO<sub>2</sub> catalysts' *Appl. Catal.*, 69, pp. 205-220.
- Kakuta, N., Tohji, K., Udagawa, Y. (1988) 'Molybdenum oxide structure on silica-supported catalysts studied by Raman spectroscopy and EXAFS', *J. Phys. Chem.*, 92, pp. 2583-2587.
- Leyrer, J., Mey, D., Knozinger, H. (1990) 'Spreading behaviour of molybdenum trioxide on alumina and silica: A Raman microscopy study', *J. Catal.*, 124, pp. 349-356.
- Leyrer, J., Zaki, M. I., Knozinger, H. (1986) 'Solid/solid interactions. Monolayer formation in molybdenum trioxide-alumina physical mixtures', *J. Phys. Chem.*, 90, pp. 4775-4780.
- Ma, X., Gong, J., Wang, S., Gao, N., Wang, D., Yang, X., He, F. (2004) 'Reactivity and surface properties of silica supported molybdenum oxide catalysts for the transesterification of dimethyl oxalate with phenol', *Catal. Commune.*, 5, pp. 101-106.
- Mathew, S., Nagy J. B., Nagaraju, N. (2006) 'Al(OH)<sub>3</sub> containing molybdenum species as an efficient support-catalyst system in benzyl alcohol reaction', *Catal. Comm.*, 7, pp. 177-183.
- Mathew, S., Kumara C. S., Nagaraju, N. (2006) 'Influence of nature of support on the catalytic activity of supported molybdenum-oxo species in benzyl alcohol conversion', *J. Mol. Catal.*, 255, pp. 243-248.
- McEvoy, T. M., Stevenson, K. J. (2005) 'Spatially Resolved Imaging of Inhomogeneous Charge Transfer Behavior in Polymorphous Molybdenum Oxide. I. Correlation of Localized Structural, Electronic, and Chemical Properties Using Conductive Probe Atomic Force Microscopy and Raman Microprobe Spectroscopy', *Langmuir*, 21, pp. 3521-3528.
- Mercera, P. D. L., Van Ommen, J. G., Doesburg, E. M. B., Burggraaf, A. J., Ross, J. B. H. (1990) 'Zirconia as a support for catalysts: Evolution of the texture and structure on calcination in air', *Appl. Catal.*, 57, pp. 127-148.
- Mulcahy, F. M., Fay, M. J., Procter, A., Houalla, M., Hercules, D. M. (1990) 'The adsorption of metal oxyanions on alumina' *J. Catal.*, 124, pp. 231-240.
- Ng, K. Y. S., E. Gulari, E. (1985) 'Molybdena on titania: I. Preparation and characterization by Raman and Fourier Transform Infrared spectroscopy', *J. Catal.*, 92, pp. 340-354.
- Sarrazin, P., Mouchel, B., Kasztelan, S. (1989) 'Molybdenum-95 NMR study of the interaction of heptamolybdate solutions with alumina and silica', *J. Phys. Chem.*, 93, pp. 904-908.
- Simionato, M., Assaf, E. M. (2003) 'Preparation and characterization of alumina-supported Co and Ag/Co catalysts', *Material Research*, 6(4), pp. 533-539.
- Smith, J. N. (1960) 'X - ray powder data file', *Amer. Soc. For Testing material*, Philadelphia, USA.
- Spanose, N., Vordonis, L., Kordulis C.H., Lycourghiotis, A., (1990) 'Molybdenum-oxo species deposited on alumina by adsorption: I. Mechanism of the Adsorption', *J. Catal.*, 124, pp. 301-314.
- Thiemann, J. P., Ressler, T., Walter, A., Muller, G. T., and Hess, C. (2011) 'Structure of molybdenum oxide supported on silica SBA-15 studied by Raman, UV-Vis and X-ray absorption spectroscopy', *Appl. Catal. A. Gen.*, 399, pp. 28-34